Journal of Sustainable Development in Africa (Volume 12, No.8, 2010)
ISSN: 1520-5509
Clarion University of Pennsylvania, Clarion, Pennsylvania

THE RELATIONSHIP BETWEEN SATELLITE DERIVED AND GROUND MEASURED SUGAR CANE WATER USE: THE CASE OF HIPPO VALLEY ESTATES IN ZIMBABWE

Matsa Mark and Muyemeki Luckson
Department of Geography & Environmental Science, Midlands State University, Zimbabwe

ABSTRACT

Effective irrigation water management can only be achieved when up to date real time information on the irrigated area, crops grown, and the levels of crop water use are available. However, the spatial scale of most irrigation schemes limit effective collection of this data, since most schemes are covering hundreds to thousands of square kilometers. The rendering of data collection is both tedious and expensive, and it limits ground based monitoring of crop performance and production estimation. Employment of remote sensing, which uses synoptic and repetitive view, may be desired to compliment ground based methods. The research seeks to determine the relationship between satellite derived sugarcane water use and ground measured sugarcane water use at the study site, Hippo Valley Estates in Zimbabwe. It explores the application of remote sensing in estimating sugar cane water use by comparing the SEBAL (Surface Energy Balance Algorithm for Land) model of estimating evapotranspiration and the ground method of measuring sugar cane water use at Hippo Valley Estates. It is hypothesized that there is no significant relationship between Landsat Thematic Mapper images of derived sugar cane water use and the ground measured sugar cane water use. The research reveals that there is a significant ($p<0.05$) positive relationship ($r=0.808466$) between ground measured sugar cane water use and the Landsat derived satellite sugar cane water use. The study also reveals that the ground based method of measuring sugar cane water use has a major limitation of assuming spatial homogeneity for the ground values measured in different sections of Hippo Valley Estates unlike the satellite derived method of estimating sugar cane water use which gives actual values of evapotranspiration on a pixel by pixel basis. It is recommended that both of these methods are used simultaneously (satellite method should be used to monitor sugar cane water use, and validation tests for the results should be used through the ground method of measuring sugar cane water use).

Keywords: Crop Water Use; Crop Factor (K)/Consumptive Use Coefficient; Remote Sensing

BACKGROUND OF STUDY

Water is a critical resource for alleviating poverty, improving human health, and food security. The increasing water scarcity and misuse of water resources presents a major threat to sustainable water management in developing countries. This continual depletion of water resources is narrowing the prospects of meeting the first goal of the Millennium Development Goals (MDGs) of eradicating poverty and hunger by 2015. With the global population expected to reach 8.1 billion by 2030, the main challenge is how to ensure the availability of water and the efficient use of this resource (Diouf, 2007).

Water is a limited and vulnerable resource, especially in southern Africa as this region is exposed to extreme climate variability and emerging climate change (Chiuta, Hirji, Johnson, & Maro, 2002). Many of the southern African countries struggle under existing water stress from pressures such as irrigation demand, industrial pollution, and water borne sewerage. Furthermore, with the emerging global climate change these pressures are likely to be significantly exacerbated. The Stockholm Environment Institute estimates that, based on only moderate climate change, by 2025 the proportion of the world's population living in countries under water stress will increase from 34% (in 1995) to 64% (WaterAid, 2007). This will lead to an increase in the world food demand as erratic weather patterns and warmer temperatures are likely to increase the threat of crop failures and food shortages.

The population of southern Africa is primarily rural based and still heavily dependent on agriculture for their welfare. There are seasonal variations and unreliable rainfall which make irrigation an essential factor for sustaining agricultural production in this region (Chiuta et al., 2002). However, irrigation is becoming an increasingly scarce resource for agriculture. At the current consumption rate of water and the increase in population, it is predicted that by 2025 two out of three people will live in drought or water stressed conditions (Tribe, 2008). According to Bandara (2006) the challenge for irrigated agriculture today is to contribute to the world's food production and to improve food security through more efficient and effective use of water. English, Soloman, and Hoffman (2002) projects that for the world to feed itself in 2025, 17% more irrigation water will be needed. This creates a tough challenge to countries in arid and semi-arid regions of southern Africa as surface and groundwater resources are naturally limited (Bouman, 2007).

The increasing water scarcity and competition for the water and land from agricultural and nonagricultural sectors drives the need to improve crop water use (evapotranspiration) so as to guarantee adequate food for future generations with the same or less water and land than that is currently available for agriculture (Platonov et al., 2008). Crop water use is a vital indicator in assessing the performance of irrigated crops. By improving crop water use, the quality and yield of crops are improved as more water is available for growing crops (Al-Kaisi & Broner, 2009).

With the increasing water scarcity within Zimbabwe there has been increased pressure on the irrigated agricultural sector to utilize less water whilst increasing food production in the country. Effective irrigation water management is only achieved when up-to-date real time information on the irrigated area, crops grown, and the levels of crop water use is available (Maxton, 2007). However, the spatial scale of most irrigation schemes limit effective collection of this data as most are vast and cover hundreds to thousands of square kilometers. In addition, there is a need for extensive personnel and financial resources to acquire such data. According to Senay, Budde, Verdin, and Melesse (2007),all this limits ground based monitoring of crop performance and production estimation. It is in the context of this background that the employment of remote sensing (using synoptic and repetitive view) becomes desirable. Remote sensing is an important tool in irrigation water management as it provides a means to accurately quantify the spatial and temporal variations in crop water use (Gowda, Chavez, Howell, Marek, & New, 2008). Despite its well known capabilities and strengths, remotely sensed crop

water use has not been applied in monitoring crop water use in Zimbabwe. The central focus is to make a comparative analysis of satellite derived crop water use with ground measured crop water use in Hippo Valley Estates.

Methods of determining crop and irrigation requirement

Ground based measurements

Traditional methods for determining evapotranspiration are based on the crop coefficient approach. Kiama (2008) states this method requires the determination of reference evaporation ($\mathbf{ET_o}$) from meteorological stations and crop coefficient ($\mathbf{k_c}$) from the look up table. Potential evapotranspiration is then determined as a product of the reference evaporation and crop coefficient. Point data $\mathbf{k_c}$ from the reference table assumes homogeneity over the respective area and may contribute to error in estimating crop water requirement due to their empirical nature (Ray & Dahwal, 2001). In view of this limitation, new techniques for estimating actual evaporation and transpiration have been developed that would potentially contribute to spatial and temporal information needed for crop water management. These techniques according to Kite and Droogers (2000) can be classified into field based, hydrological models, and remote sensing methods, each fit for different circumstances.

Remote sensing methods

According to Wesseling and Feddes (2006) remote sensing allows for independent observation of actual situations on spatial variability of vegetation. The basis of its application in quantifying spatio-temporal variation in water use is in its ability to discriminate land features and variations in important crop parameters, such as evapotranspiration (Bandara, 2006). Existing methods applied to derive parameters and performance indicators from spectral reflectance measurements vary in data requirements related to their use. One method includes the use of advanced remote sensing flux algorithms which have been developed over the last few decades to estimate actual evapotranspiration. These algorithms differ in the procedure employed to resolve the energy balance equation; some calculate the sensible heat flux first and then obtain the latent heat flux as the residual of energy balance equation, while others estimate the relative evaporation by means of an index using a combination equation (Kiama, 2008). These include the Surface Energy Balance Algorithm for Land (SEBAL), Crop Water Stress Index, Surface Energy Balance Index (SEBI), and Surface Energy Balance System (SEBS). These have been tested successfully.

Apart from the flux algorithms, canopy reflectance based approach has proved to be rather simple and straightforward technique in estimating evapotranspiration. An example is Bausch (1995) who used the soil adjusted vegetation index (SAVI) to evaluate the performance of canopy reflectance based crop coefficient as an effective indicator of irrigation scheduling for corn. A linear transformation between basal crop coefficient ($\mathbf{k_{cb}}$) and the SAVI was used to convert SAVI into crop coefficient ($\mathbf{k_{cr}}$).

Some aspects of these methods need to be improved. There is a need to account for the differential spectral reflectance between wet and dry soil, which is a limitation of canopy reflectance based crop coefficient method (Choudhury, Ahmed, Idso, Reginato, & Daughtry, 1994). According to Kiama (2008) the other challenge relates to the resolution of available remote sensing data. High temporal resolution sensors have coarse sparse resolution that does not fit the application of field level irrigation scheduling.

DESCRIPTION OF STUDY AREA

Hippo Valley Estates are sugar cane estates found near the town of Chiredzi in Chiredzi District of southeastern Zimbabwe, on the Runde River. The sugar plantation falls under agro-eco region 5. The area receives erratic rainfall which is below 450mm per year with temperature ranging from 25° C to 27.5° C (77 ^{o} F to 81.5^{o} F). In October temperatures may rise as high as 40° Celsius (104 ^{o} F).

Hippo Valley Estates was established in 1956 as citrus estates. Although, it was established as citrus fruit estates, Hippo Valley Estates diversified into sugar cane growing and the first cane was planted in 1969. In 1975 following the crash in the citrus market, Hippo Valley Estates moved its focus to irrigated cane growing. Today, Hippo Valley Estates is one the two major producers of sugar in Zimbabwe; the other being Triangle Limited. The two estates also have a fifty fifty share in Mkwasine Estate, which is located north east of Hippo Valley Estates. The sugar plantation covers over 124 square kilometers and the company employs around 5,000, mostly from Chiredzi Town.

The estate operations cover an area of approximately 54,205 hectares. Approximately 15,466 hectares are under cane, forestry plantations, citrus, and other crops. A large proportion of the estate (25,874 hectares) is under cattle and game ranching. The remainder of the land use is split as follows: major dams (113 ha), developed areas (2,237 ha) major roads, railways, airstrip, and Naude (747 ha), and finally land unsuitable for cultivation including major river frontages (8,768 ha).

Hippo Valley Estates have a capacity of 300,000 tonnes of sugar per year. The product range is mostly raw sugar, brown sugar (sun sweet), and refined sugar. Figure 1 (below) shows a map of Hippo Valley Estates.

Figure 1: Map of Hippo Valley Estates

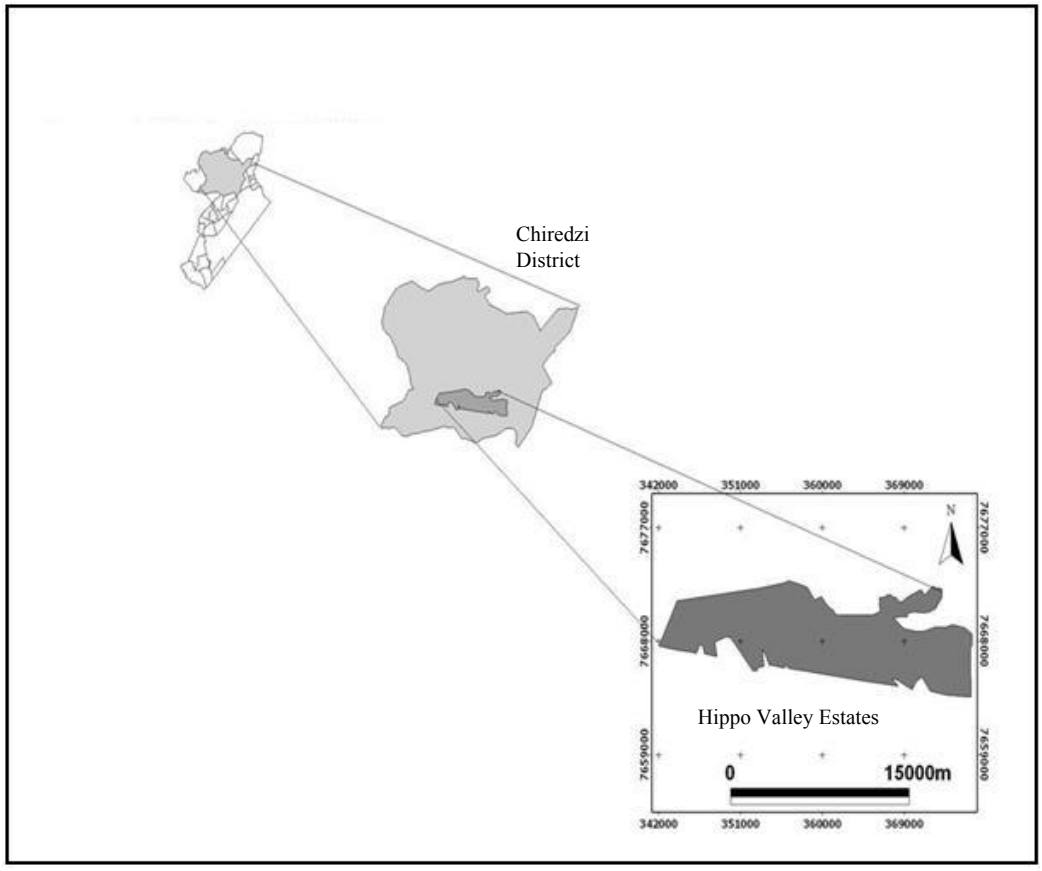

MATERIALS AND METHODS

Methods of Data Collection

Data inputs

A Landsat ETM+ image was used to calculate sugar cane water use. The satellite imagery data was obtained from the Global Land Cover Facility (GLCF) on Earth Science Data Interface on the Internet (http://www.glcf.umiacs.umd.edu.8080/esdi/index/jsp). Additional data include meteorological data on Hippo Valley.

Table 1: Satellite Data Acquired for Study

Satellite sensor	Path/Row	Acquisition date
Landsat 7 Thematic Mapper (TM)	169/074	19 May 2006

Pre-processing of images

The image was georeferenced to WGS-1984 UTM coordinate system so that the image coordinates are in line with the ground coordinates. Radiometric corrections were also carried out to remove haze within the images. The image was then calibrated in which the DN (Digital Numbers) values or QCAL (quantified and calibrated values) of the image bands were converted to radiance as radiance values are required in estimating evapotranspiration.

Calculation of sugar cane water use using satellite images

The SEBAL (Surface Energy Balance Algorithm for Land) approach was used to make spatial estimates of evapotranspiration so as to calculate sugar cane water use. This was carried out in ILWIS 3.4

SEBAL is an image processing model that calculates evapotranspiration as the residual of an energy balance applied to the land surface for each pixel of a satellite image. It is calculated using the following equation:

$$\lambda E = R_n - G - H \quad (1)$$

Where:

λE (Wm^{-2}) is the latent heat flux,

R_n (Wm^{-2}) is the net radiation,

G (Wm^{-2}) is the soil heat flux density,

H (Wm^{-2}) is the sensible heat flux.

Calculation of Net Radiation

Net radiation (R_n) is the sum of the incoming and outgoing shortwave and longwave radiation. It is computed from solar radiation, surface albedo, NDVI and surface temperature. Net radiation is calculated using the land surface radiation balance as shown below:

$$R_n = (1-\alpha)R_s + (\varepsilon L_{in} - L_{out}) \quad (2)$$

Where:

α is surface albedo,

R_s is solar radiation,

ε is surface emissivity,

L_{in} is incoming radiation,

L_{out} is outgoing radiation.

In this study net radiation was computed as the difference between the net shortwave radiation and net longwave radiation which is shown below:

$$\mathbf{R_n = S\Delta + L\Delta} \quad (3)$$

Where:

SΔ is net shortwave radiation,

LΔ is the net longwave radiation.

$$\mathbf{S\Delta = (1\alpha)S\downarrow}$$

(4)

Where:

S↓ is the incoming shortwave radiation.

$$L\Delta = \sigma\varepsilon_a T_a^4 - (1-\varepsilon_o)\,\varepsilon_a \sigma T_s^4 - \varepsilon_o \sigma\, T_s^4$$

(5)

Where:

σ is the Stefan-Boltzmann constant which is taken as 5.67×10^{-8},

ε_a is emissivity of the atmosphere,

ε_o is the surface emissivity,

T_a is the air temperature,

T_s is the land surface temperature.

Figure 2: Net Radiation (Wm^{-2}) Map for Hippo Valley Estates (Field Data)

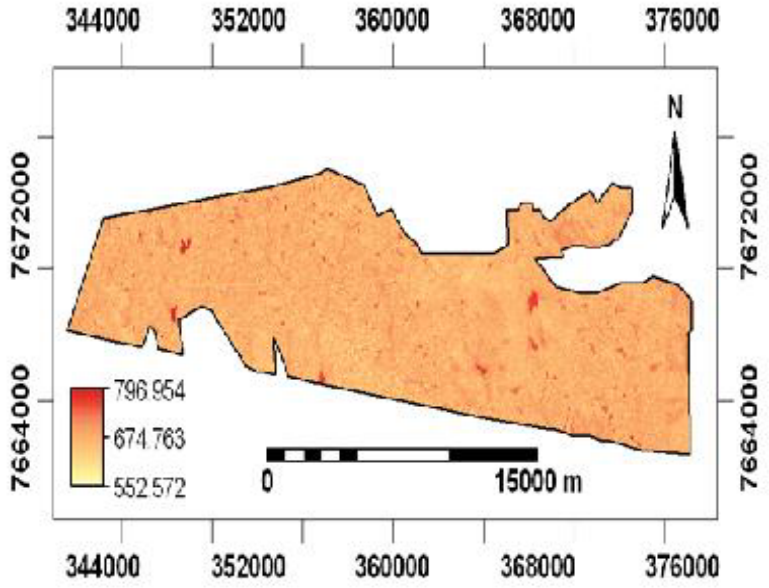

The variables required in the computation of Net radiation which are surface albedo, surface emissivity, NDVI, and surface temperature were calculated as follows:

a) Calculation of surface albedo

Land surface albedo is a physical parameter that describes the optical reflectance of land surface (Duguay & Leowe, 1991; Maurer, 2006). Remote sensing instruments do not directly measure surface albedo. As a result, albedo was inferred through a series of manipulations to the raw remote sensing data. Firstly, the effective at-satellite reflectance or planetary albedo, Pp, was calculated as according to Markham and Barker (1986):

$$\rho_p = \frac{\pi \cdot L_\lambda \cdot d^2}{ESUN_\lambda \cdot \cos\theta_s}$$

(6)

Where:

Pρ = effective at-satellite planetary reflectance composed the combined surface and atmospheric reflectance of the earth (unitless),

L_λ = spectral radiance at sensor (in mW cm^{-2} $ster^{-1}m^{-1}$),

d = Earth-Sun distance in astronomical units,

Esun (λ) = mean solar exoatmospheric irradiances (in mW cm^{-2} $ster^{-1}m^{-1}$),

$\cos\theta_s$ = solar zenith angle (in degrees), given on the header of the image, π = 3.1416.

The updated mean solar exoatmospheric irradiances, E_{sun} (λ), from Markham and Barker (1986) are given in Table 2.

Table 2: Solar Exoatmospheric Spectral Irradiances for the TM Bands

TM BAND	**F**
TM 1	195.58
TM 2	182.8
TM 3	155.9
TM 4	104.5
TM5	21.91
TM7	7.457

Source: Markham and Barker (1986)

The Earth-Sun distance, d, was approximated as

$$d=1+0.0167\sin[2\pi (D-93.5)/365)$$

(7)

Where:

d is the day number of the year.

In the present study a pre-defined algorithm in ENVI (Environment for Image Analyst) was run to convert DN values into exoatmospheric reflectance (reflectance above the atmosphere) values. Land surface albedo was then calculated following Wang et al (2000).

$$\alpha =0.221*B1+0.162*B2 +0.102*B3 + 0.354*B4 +0.068*B4 +0.059*B5 +0.0195*B7$$

(8)

Where:

B1 to B7 are effective at-satellite reflectance at nadir from Landsat TM band 1 to band 7.

Figure 3: Albedo Map for Hippo Valley Estates (Field Data)

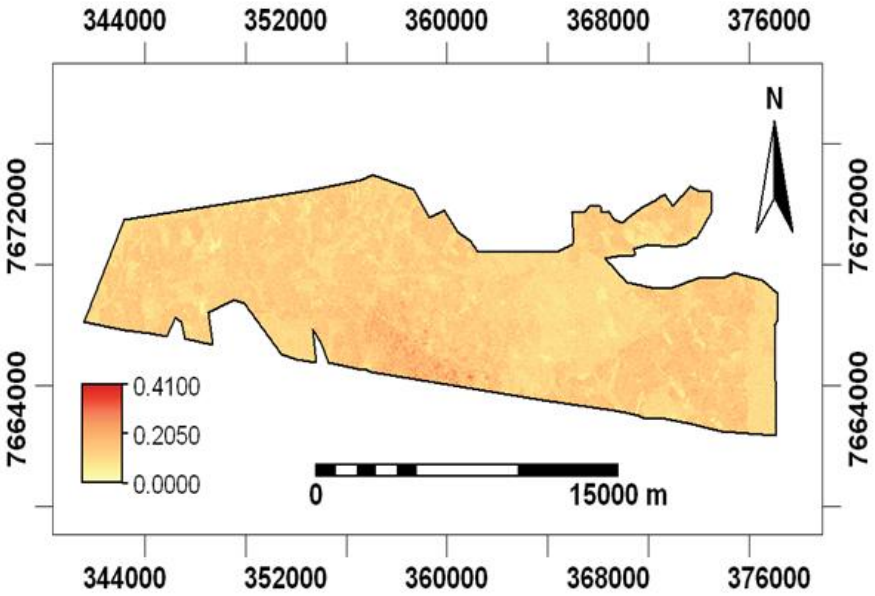

(b) Calculation of surface emissivity

Surface emissivity is the efficiency with which the surface emits longwave radiation at a given temperature in the 3 to 100μm spectral range (Maxton, 2007). Surface emissivity was calculated using the following algorithm:

$$\varepsilon_o = 1.009+0.047 \ln (NDVI) \quad (9)$$

Where:

ε_o= surface emissivity,

ln= natural logarithm,

NDVI= Normalized Difference Vegetation Index.

Figure 4: Surface Emissivity Map for Hippo Valley Estates (Field Data)

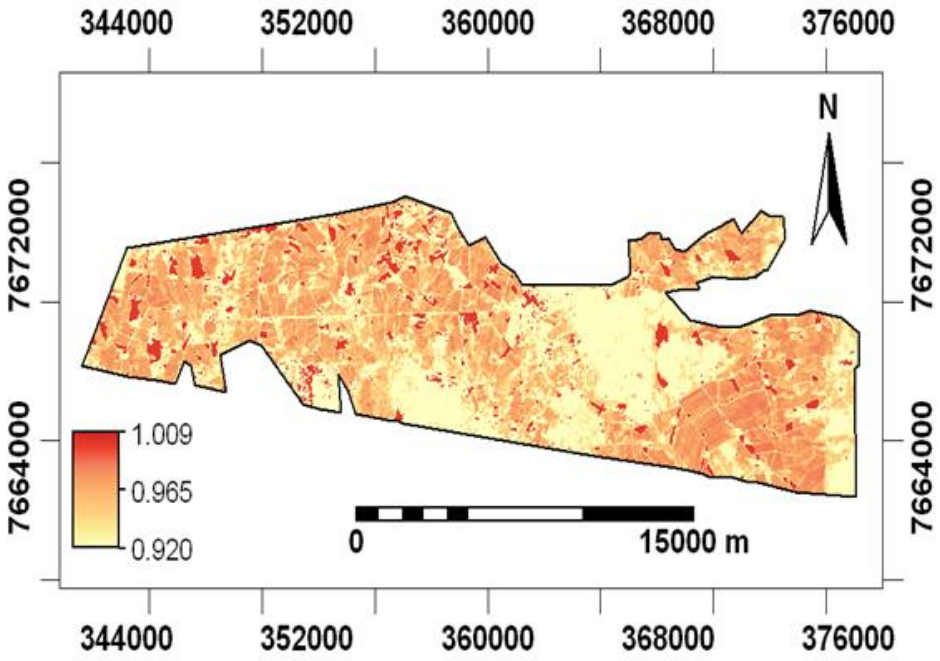

(c) Calculation of NDVI

NDVI (Normalized Difference Vegetation Index) is an index used to measure the presence and condition of green vegetation. NDVI was calculated using following equation:

$$NDVI = \frac{NIR-R}{NIR+R} \quad (10)$$

Where:

NIR= near infra-red band,

R = red band.

Figure 5: NDVI Map for Hippo Valley Estates (Field Data)

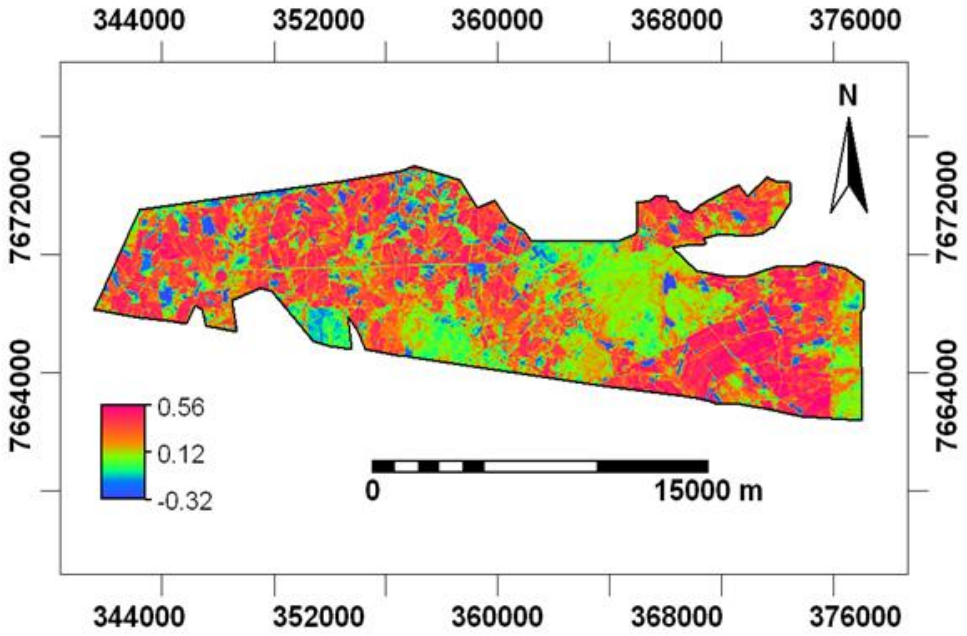

(d) Calculation of Land surface temperature

Radiance converted from the (QCALs) do not represent a true surface temperature but a mixed signal of different signals of energy. Land surface temperature was calculated in two steps:

(1) The effective at-satellite temperature (T) using the following equation:

$$T = \frac{K1}{\ln((K2/L+1)) - 273)} \ (^{o}\mathrm{C}) \tag{11}$$

Where:

ln= natural logarithm,

T= effective at-satellite temperature in Kelvin,

K2= thermal calibration constant (1260.56),

K1= thermal calibration constant (60.776),

L= spectral radiance of band 6 in watts/(meter squared * ster * μm).

(2) Studies by Timmermans (1994) found that it is not necessary to apply an atmospheric correction for Landsat Thermal imagery and so it can be assumed that the Effective at-satellite temperature and at the surface are equal (T=TEMPSUR). The land surface blackbody temperature map was then corrected for emissivity to give a grey body land surface temperature map.

$$To = \left((TEMPSUR + 273)^4 / \varepsilon_o\right)^{0.25} \ [Kelvins] \tag{12}$$

Where:

TEMPSUR=land surface temperature.

Figure 6: Surface Temperature (K) Map for Hippo Valley Estates (Field Data)

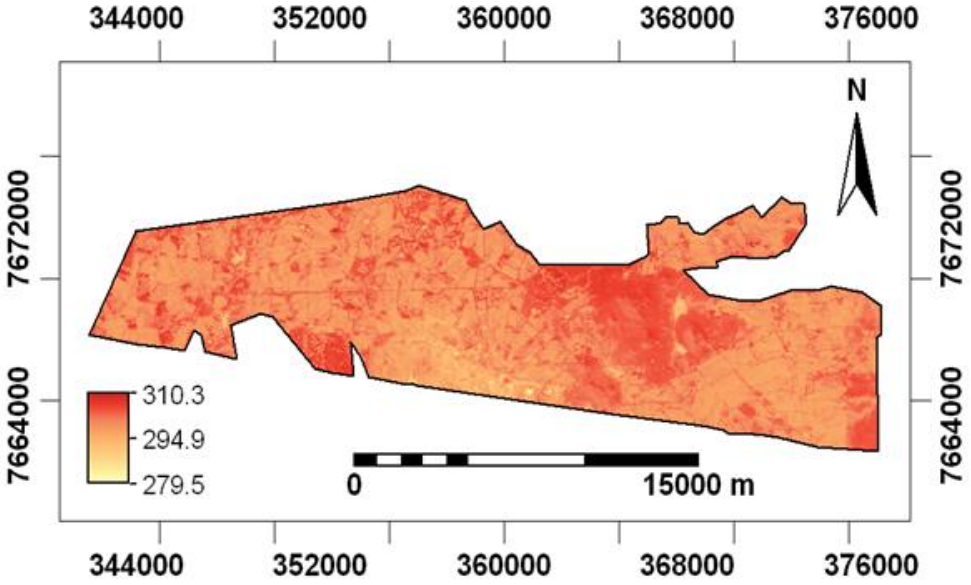

Calculation of the soil heat flux

Soil heat flux (G) is the heat that is transported through the soil by conduction and convection. It is empirically estimated using a function by Bastiaanssen (2000) based on net radiation, albedo, surface temperature and normalized difference vegetation index (NDVI):

$$G = \left[\frac{T_s - 273.16}{\alpha} (0.0038\alpha + 0.0074\alpha^2)(1 - 0.98NDVI^4) \right] R_n \quad (13)$$

Where:

T_s is the land surface temperature,

α is the surface albedo,

R_n is the net radiation,

NDVI is the Normalized Vegetation Index.

Figure 7: Soil Heat Flux (Wm^{-2}) Map for Hippo Valley Estates (Field Data)

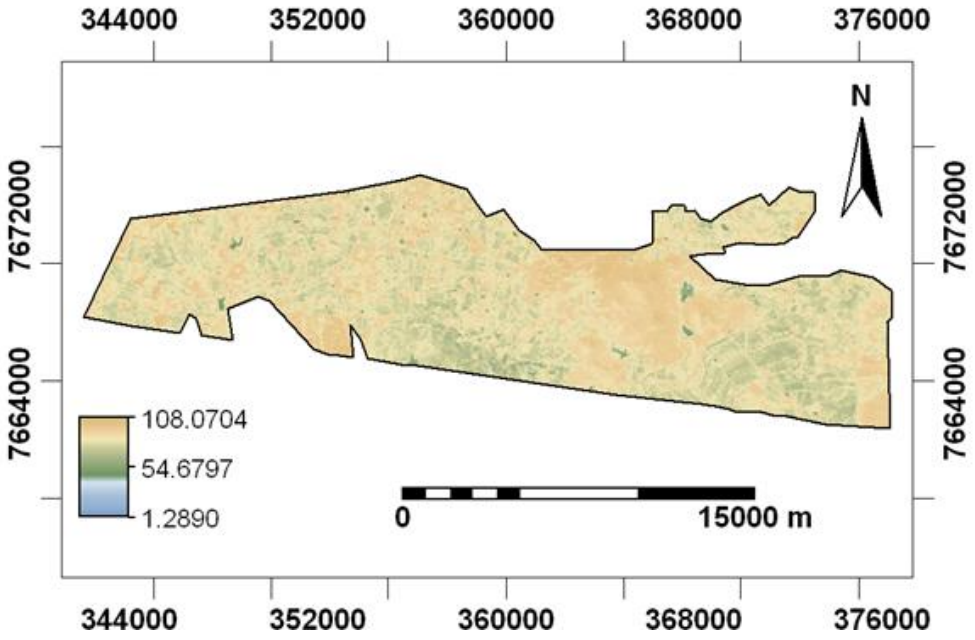

Calculation of the sensible heat flux

The sensible heat flux (H) is the flow of energy through the air as a result of the temperature gradient. Since the land surface temperature during the day is usually much higher than the air temperature, the sensible heat flux is normally directed upwards during the day. It is estimated from wind speed and surface temperature using a unique "internal calibration" of the near surface to air temperature difference (dT) as described by Bastiaanssen, Noordman, Pelgrum, Davids, and Allen (2003):

$$H = \frac{\rho_{air} C_p (a + b \cdot T_s)}{r_{ah}} \quad (14)$$

Where:

P_{air} is air density is a function of atmospheric pressure,

C_p is the specific heat capacity of air (≈ 1004 J $kg^{-1}K^{-1}$),

r_{ah} is aerodynamic resistance to heat transport(s m^{-1}),

T_s is surface temperature (Kelvins),

a is an empirical coefficient calibrated for the image,

b is an empirical coefficients calibrated for the image.

The term "$a+bT_s$" in the equation represents the near surface temperature (Ts) to air temperature (Ta) difference which is commonly represented as dT. It is computed between a height near the surface and a height about 2m. Use of air difference (i.e. gradient), eliminates problems caused by difference between radiometric and aerodynamic surface temperature.

In order to calculate the sensible heat flux following steps are required: there is first the need for the selection of both the dry and wet pixel. This is then followed by the estimation of the empirical coefficients a and b. The near surface temperature to air temperature difference (dT). This resultant difference in the near surface temperature to air temperature is then used as an input in the computation of the sensible heat flux.

a) Selection of the dry and wet pixel for the determination of dT

The researcher selected the dry pixel based on the temperature-albedo relationship. The pixel with low albedo and high temperature is selected as the dry pixel. The wet pixel was selected based on the NDVI-temperature relationship. Usually a pixel with low NDVI and low temperature is selected as the wet pixel. For the wet pixel it is assumed that the sensible heat flux is zero. Therefore according to this assumption the near surface to air temperature difference for the wet pixel (dTwet) is also equal to zero. For the dry pixel the condition is that dTdry= dTmax. The near surface to air temperature difference for the dry pixel (dTdry) was estimated at 13.5699 K.

Table 3: Derived Components of the Dry and Wet Pixel for Hippo Valley Estates (Primary Data)

	Dry Pixel	**Wet Pixel**
Location	370101.43E, 7671429.13S	361501.81E, 7665670.48S
Derived Components		
Net Radiation	643.512	749.024
Soil Heat Flux	105.4472	40.8726
Surface Temperature	309.8	289.5
NDVI	-0.1	0.73
Albedo	0.0909	0.1118

Figures 8 and 9 (below) are the scatter plots for the determination of the dry and wet pixel.

Figure 8: Scatter Plot between Albedo and Surface Temperature for the Determination of the Dry Pixel (Primary Data)

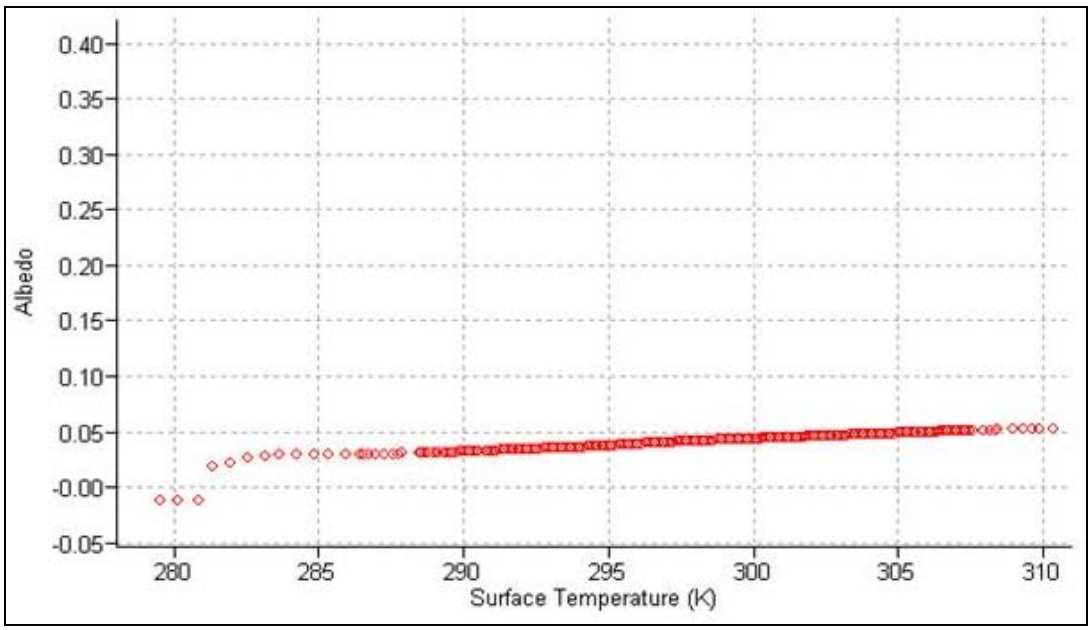

b) Estimation of constants a and b for the determination of dT

The estimation of the constants **a** and **b** was done by determining the linear relationship between dT and surface temperature. The value of constants **a** and **b** were computed as -193.52 and 0.6685, respectively. Table 4 shows the components used in the computation of constants **a** and **b**:

Table 4: Derived Components for the Estimation of Constants a and b (Primary Data)

Surface Temperature(K)	**dT(K)**
289.5	0
309.8	13.5699

Figure 9: Scatter Plot between NDVI and Surface Temperature for the Determination of the Wet Pixel (Primary Data)

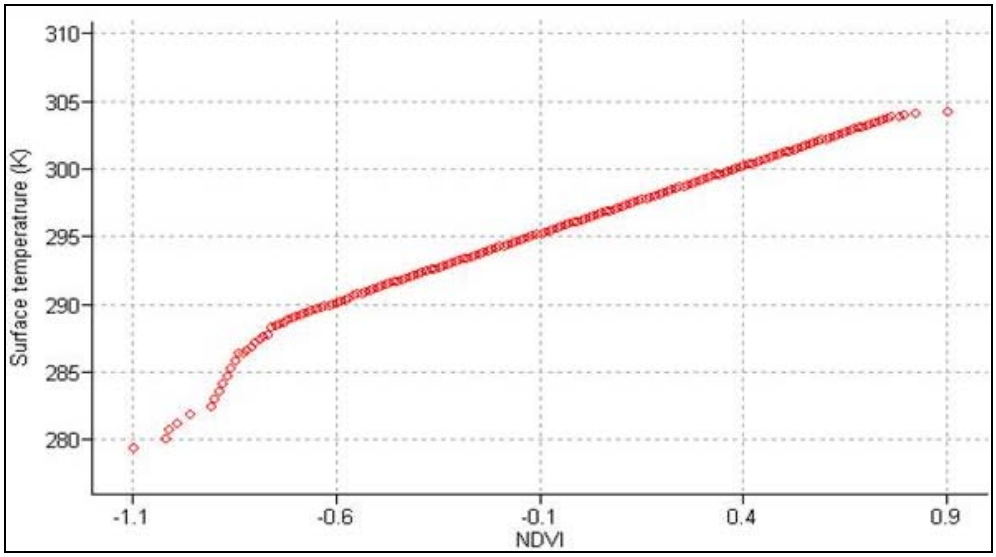

Figure 10: Plot of dT Over Surface Temperature for Determining the Constants a and b (Primary Data)

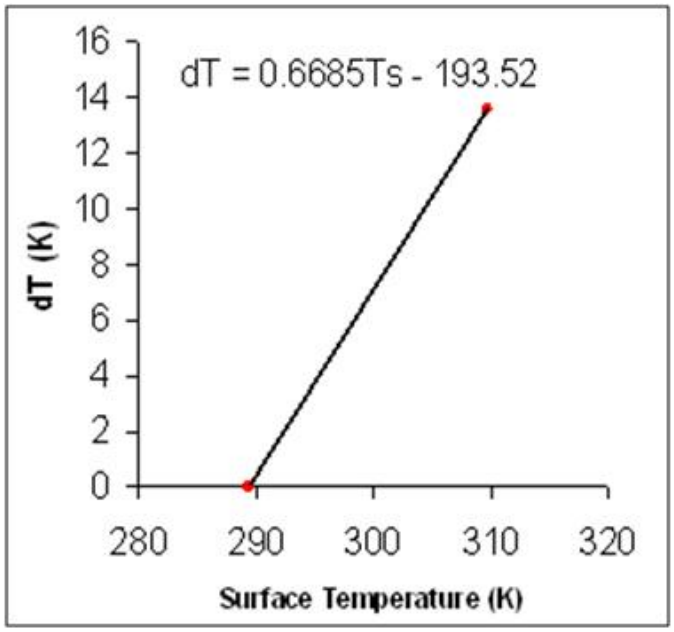

Using the values of constants **a** and **b** computed in the above process a map of the difference in surface and air temperature (dT) was developed as shown in Figure 10, above.

Figure 11: Map Showing the Difference between Surface and Air Temperature (K) for Hippo Valley (Field Data)

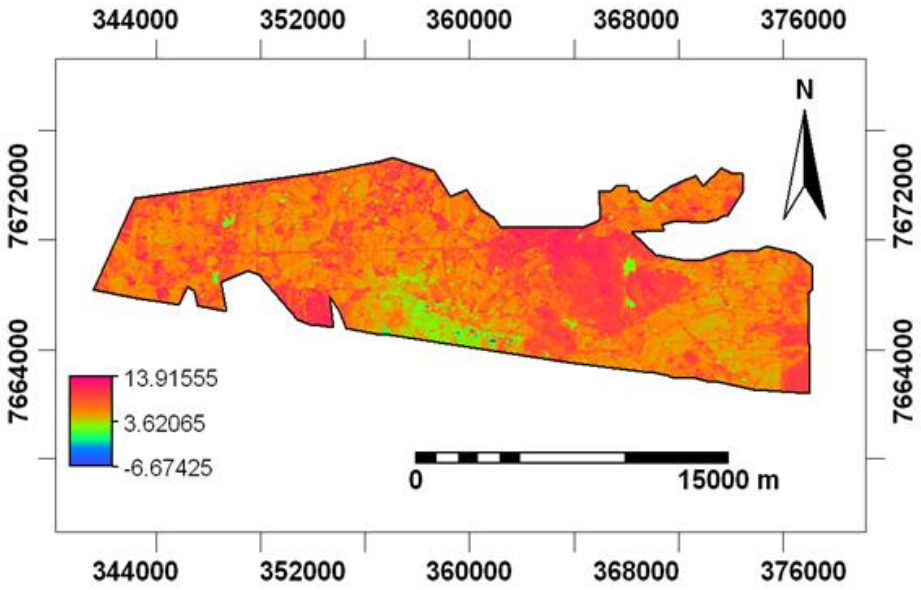

The dT map was then used as an input in the calculation of the sensible heat flux. The resultant sensible heat flux is shown on Figure 12, below.

Figure 12: Sensible Heat Flux Map (Wm^{-2}) for Hippo Valley Estates (Field Data)

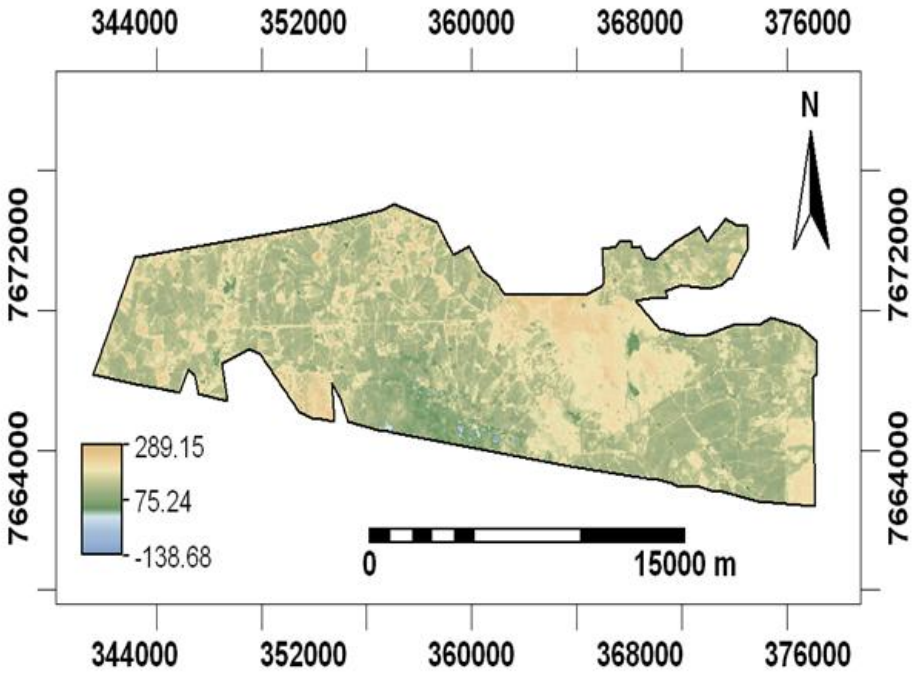

Calculation of the latent heat flux

After the estimation of net radiation, soil heat flux and the sensible heat flux, the latent heat flux was then calculated as a residual term of the energy balance equation shown below:

$$\lambda E = R_n - G - H \tag{15}$$

Where:

λE (Wm^{-2}) is the latent heat flux,

R_n (Wm^{-2}) is the net radiation,

G (Wm^{-2}) is the soil heat flux,

H (Wm^{-2}) is the sensible heat flux.

Figure 13: Latent Heat Flux (Wm^{-2}) Map for Hippo Valley Estates (Field Data)

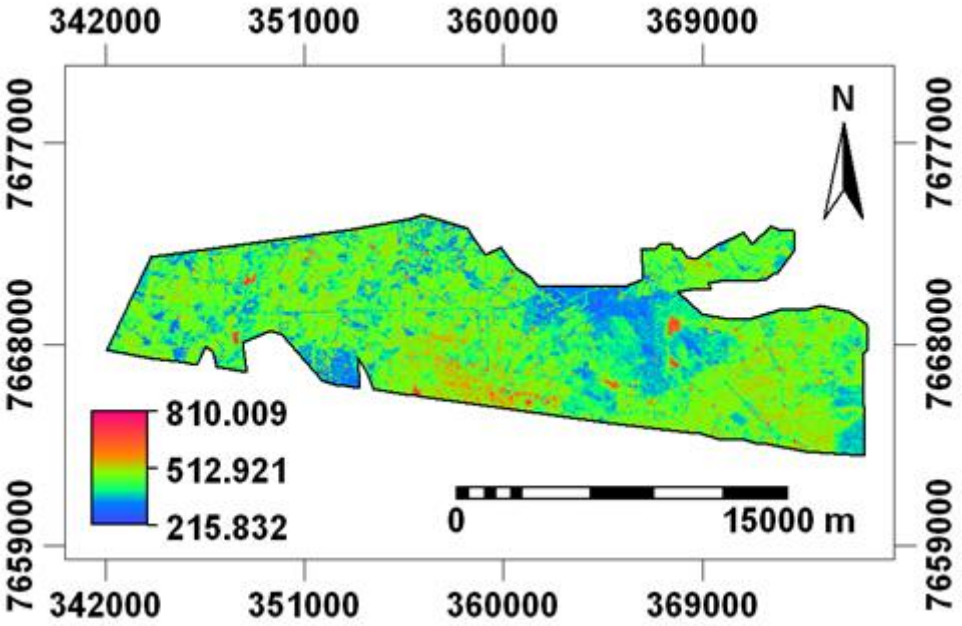

Calculation of daily evapotranspiration

Having calculated the latent heat flux, daily evapotranspiration for Hippo Valley Estates was then calculated using the following equation:

$$ET_{day} = \frac{\Lambda \times R_{n-day}}{28.588} \tag{16}$$

Where:

ET_{day}= daily evapotranspiration,

Λ= evaporative fraction,

$R_{n\text{-}day}$= daily net radiation,

In order to calculate the daily evapotranspiration the Evaporative fraction and the daily net radiation have to be first computed.

(a) Calculation of the Evaporative Fraction

The Evaporative Fraction is the fraction of energy available for evapotranspiration at the time of satellite overpass. This is an important component in the estimation of daily evapotranspiration and average monthly evapotranspiration. The Evaporative Fraction was determined by the following algorithm:

$$\Lambda = \frac{\lambda E}{R_n - G} \quad (17)$$

Where:

λE (Wm^{-2}) is the latent heat flux,

R_n (Wm^{-2}) is the net radiation,

G (Wm^{-2}) is the soil heat flux.

Figure 14: Map Showing the Evaporative Fraction for Hippo Valley Estates (Field Data)

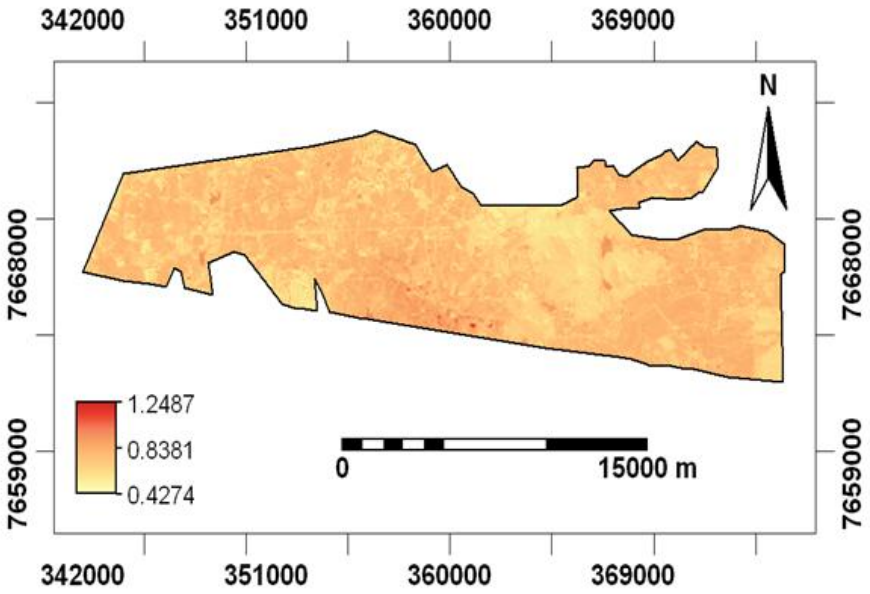

(b) Calculation of daily net radiation

The daily net radiation was calculated using the following equation:

$$R_{n\text{-}day}=(1\text{-}1.1\times\alpha)S\downarrow_{day}+L_{day} \quad (18)$$

Where:

$R_{n\text{-}day}$ is the daily net radiation,

$S\downarrow_{day}$ is the average daily incoming short wave radiation,

L_{day} is the average net long wave radiation.

Figure 15: Daily Net Radiation (Wm^{-2}) Map for Hippo Valley Estates (Field Data)

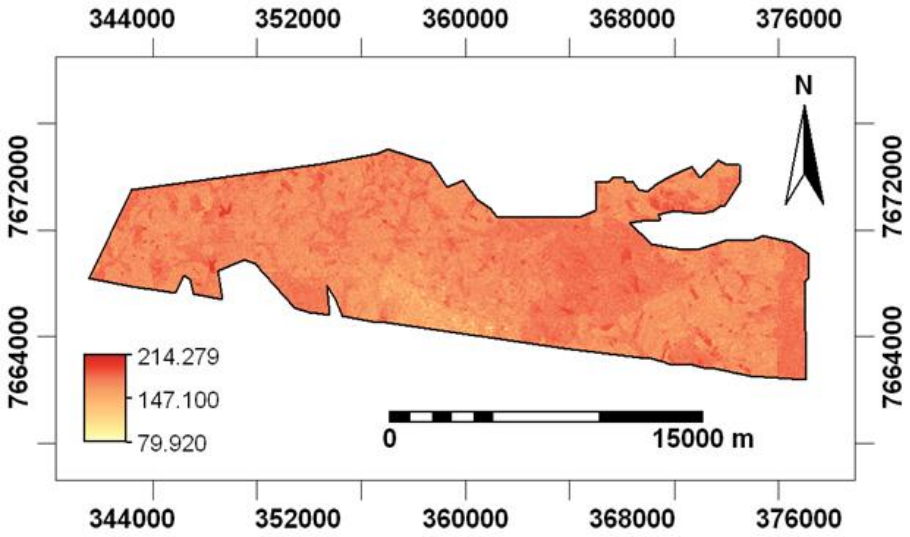

Determination of sugar cane water use using ground measurements

a) Key respondents

Three interviews were carried out with the goal of unearthing the existing method of measuring sugar cane water use that is implemented in Hippo Valley Estates. The key respondents included the Assistant Agronomist (Mr. Maronga), as he is responsible for monitoring crop performance. The Assistant Irrigation Engineer (Mr. Chamisa) was also interviewed as he is responsible for monitoring sugar cane water use. The Section Manager (Mr. Mavhundutsa) was interviewed, since he is responsible for ensuring that all the instructions coming from the Irrigation Engineer and Agronomist are implemented in the sugar cane fields. These authorities provided relevant information on the method used in measuring sugar cane water use, as well as the merits and demerits of the method used in measuring sugar cane water use.

b) Secondary data collection

In order to acquire the ground values for sugar cane water use the researcher used purposive sampling in which the researchers used the centroid locations of Section 5, Section 26, and ZSA (Zimbabwe Sugar Cane Association) as sample sites to collect ground data. The ground values for sugar cane water use for May 19, 2006 were collected using existing

records from Section 5, Section 26, and ZSA so that these values will be compared with the satellite derived sugar cane water use values for May 19, 2006.

Since the ground values acquired from each of the sample sites are assumed to be homogeneous throughout each of the sections (Section 5, Section 26, and ZSA) by the relevant authorities (Assistant Agronomist, Assistant Irrigation Engineer, and Section Manager) who measure sugar cane water use, the researchers therefore generated random points for Section 5, Section 26, and ZSA using Geographic Information Systems(GIS) to compare the sugar cane water use values for these points on the satellite image with the values on the ground. The resultant comparison was then evaluated with the initial comparison between the ground values for sugar cane water use and the satellite values for sugar cane water use to assess if there is any significant difference between the two. This helped in validating if the satellite derived method of estimating sugar cane water use is an appropriate method for measuring sugar cane water use.

DATA ANALYSIS

Testing for Normality in Satellite Derived Sugar Cane Water Use

The data was tested for normality. It was hypothesized that the sugar cane water use data does not significantly (α=0.05) deviate from a normal distribution.

H_o: The data on sugar cane water use is not normal

A Kolmogorov-Smirnov test was used and it revealed that the data does not significantly (p (sugar cane water use) =0.058; α=0.05) deviate from a normal distribution. Parametric tests were therefore used in this study.

Correlation Tests

The data was tested to determine whether there is a significant relationship between satellite derived sugar cane water use and ground measured sugar cane water use. It was hypothesized that there is no relationship between satellite derived sugar cane water use and ground measured sugar cane water use.

H_o: r=0 (there is no relationship)

The Pearson's correlation coefficient test was used to determine if there is a significant relationship between satellite derived sugar cane water use and ground measured sugar cane water use, as it is a parametric test.

RESULTS AND DISCUSSIONS

The Relationship between Satellite Derived Sugar Cane Water Use and Ground Measured Sugar Cane Water Use

Figure 16 illustrates the relationship between ground measured sugar cane water use and Landsat derived sugar cane water use. It can be observed that there is a positive relationship (r=0.91898) between ground measured sugar cane water use and the Landsat derived satellite sugar cane water use.

Figure 16: Relationship between Ground Measured Sugar Cane Water Use and Landsat Derived Sugar Cane Water Use

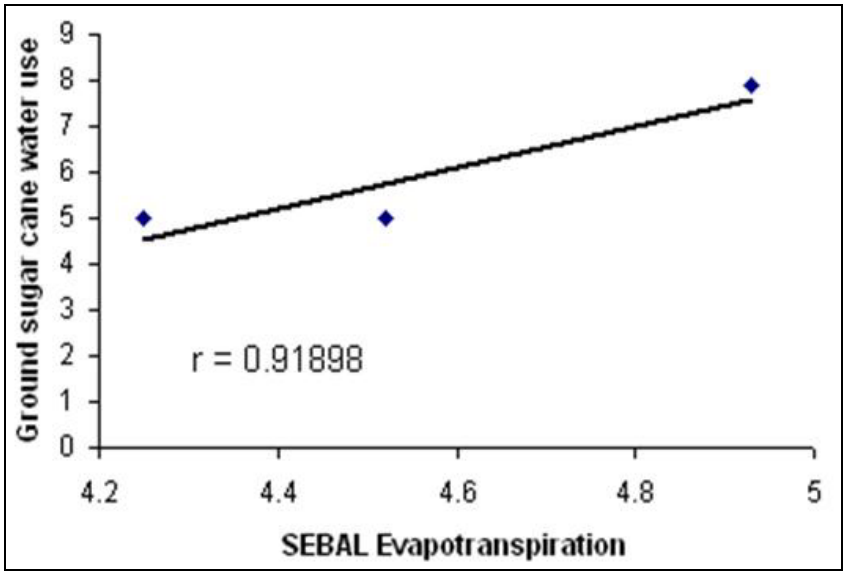

This clearly indicates that satellite derived sugar cane water use can be used in monitoring sugar cane water use especially over large areas like Hippo Valley Estates as shown in Figure 16, above.

Figure 17: Relationship between Ground Measured Sugar Cane Water Use and Landsat Derived Sugar cane Water Use Using GIS Generated Random Points

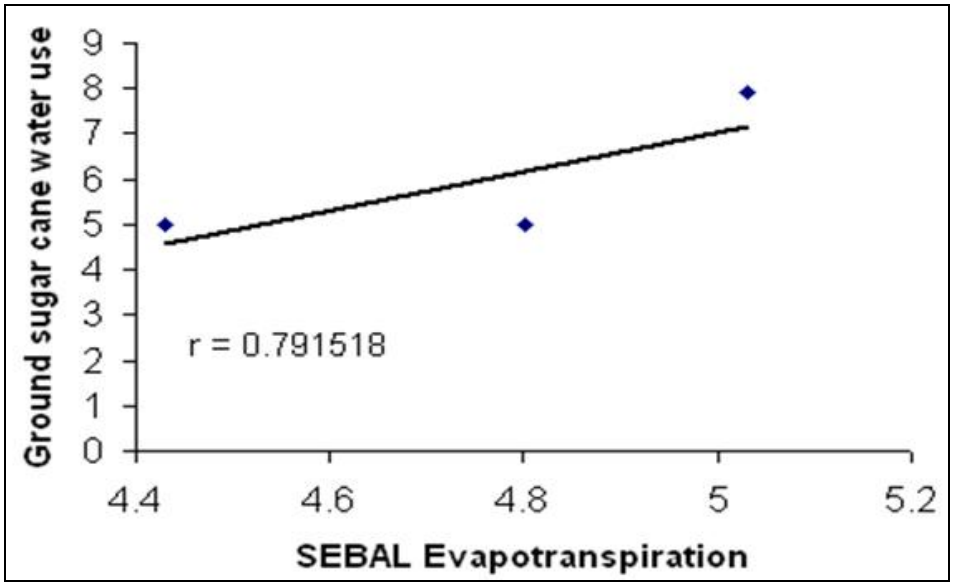

The correlation graph observed in Figure 17 (above) shows that the correlation coefficient has slightly reduced to 0.791518, however there still remains a positive relationship between ground measured sugar cane water use and satellite derived sugar cane water use meaning that satellite derived sugar cane water use can be used in monitoring sugar cane water use. In

comparison with Figure 16, this difference in the correlation coefficients indicates that the assumption by the relevant authorities (Assistant Agronomist, Assistant Irrigation Engineer, and Section Manager) who measure sugar cane water use that each of the values of sugar cane water use is homogeneous throughout each section (section 5, section 26, and ZSA) is wrong as there is an element of heterogeneity which is indicated by the difference in correlation coefficients between Figures 16 and 17.

Figure 18: Relationship between Ground Measured Sugar Cane Water Use and Landsat Derived Sugar Cane Water Use Using Both GIS Generated Random Points and the Original Centroid Points

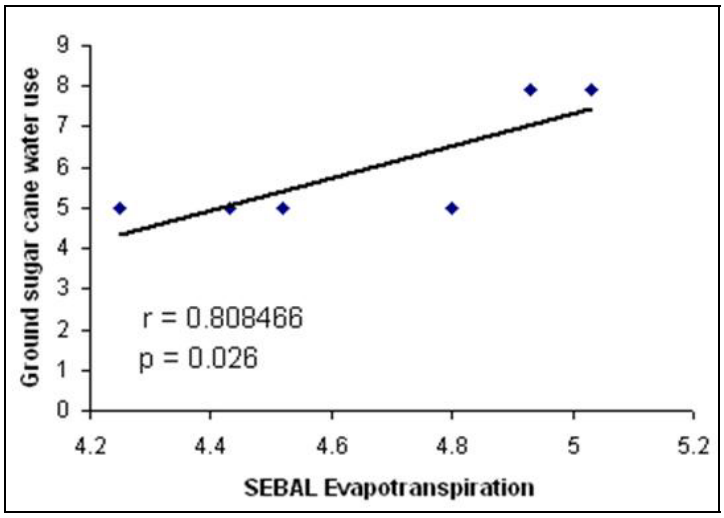

Figure 18 shows a correlation graph using both points from Figures 16 and 17. The high correlation coefficient of 0.808466 observed in Figure 18 clearly indicates that satellite derived sugar cane water use can be used in monitoring sugar cane water use as there is a significant ($p<0.05$) positive relationship ($r=0.808466$) between ground measured sugar cane water use and satellite derived sugar cane water use.

CONCLUSIONS AND RECOMMENDATIONS

This study sought to determine the relationship between satellite derived sugar cane water use and ground based sugarcane water use at Hippo Valley Estates. The study reveals that there is a positive relationship ($p<0.05$) between ground measured sugarcane water use and the Landsat derived satellite sugarcane water use. Satellite derived sugarcane water use can therefore be used in monitoring sugarcane water use especially over large areas like Hippo Valley Estates. However, the number of points used for correlation was a limiting factor to correlation tests. There is need to sample a larger number of ground points so as to attain more accurate test results.

Basing on the finding from this research, the following recommendations are suggested:

- Both ground based and satellite derived methods of measuring sugar cane water use should be used at Hippo Valley in monitoring and assessing sugar cane water use as they complement one another.

- Satellite derived methods of measuring sugar cane water use should be used to estimate sugar cane water use on a pixel to pixel basis while the ground methods should be used to validate the results from satellite images.
- For the ground methods to be used more effectively, it is recommended that more evaporation pans be distributed over the Estates so that more ground data on sugar cane water use is obtained. In this study only three points were used in correlation analysis due to inadequate data.

REFERENCES

Al-Kaisi, M. M., & Broner, I. (2009). *Crop water use and growth stages*. Retrieved from http://www.ext.colostate.edu/pus/Crops/04715.html

Bandara, K. M. P. S. (2006). *Assessing irrigation performance by using remote sensing* (Master's Thesis). ITC Wageningen University, Wageningen, The Netherlands.

Bastiaansseen, W. M. G. (2000). SEBAL-based sensible and latent heat fluxes in the irrigated Gediz Basin, Turkey. *Journal of Hydrology*, *229*(1), 87-100.

Bastiaansseen, W. M. G., Noordman, E. J. M., Pelgrum, H., Davids, G., & Allen, R. G. (2003). SEBAL for spatially distributed Evapotranspiration under actual management and growing conditions. *Journal of Irrigation and Drainage Engineering*, *221*(3), 78-91.

Bausch, W. C. (1995). Remote sensing of crop coefficients for improving the irrigation scheduling of corn. *Agricultural Water Management*, *27*(1), 55-68. Citied in S. M. Kiama (2008), *Exploring application of remote sensing in estimating crop evapotranspiration: Comparison of S-SEBI algorithm and adapted FAO56 model using Landsat TM5 and MODIS* (Master's thesis). ITC Wageningen University, Wageningen, The Netherlands.

Bouman, B. A. M. (2007). A conceptual framework for the improvement of crop water productivity at different scales. *Agricultural Systems*, *93*(1), 43-60.

Choudhury, B., Ahmed, N., Idso, S., Reginato, R., & Daughtry, C. S. T. (1994). Relations between evaporation coefficients and vegetation indices studied by model simulations. *Remote Sensing of the Environment*, *50*(1), 1-17. Citied in S. M. Kiama (2008), *Exploring application of remote sensing in estimating crop evapotranspiration: Comparison of S-SEBI algorithm and adapted FAO56 model using Landsat TM5 and MODIS* (Master's thesis). ITC Wageningen University, Wageningen, The Netherlands.

Chiuta, T., Hirji, R., Johnson, P., & Maro, P. (2002). *Defining and mainstreaming environmental sustainability in water resources management in Southern Africa.* Harare, Zimbabwe: Southern Africa Research and Documentation Centre (SARDC).

Diouf, F. W, Donkor, S. M. K., & Yilma, W. E. (1999). *Integrated water resource management in Africa: Issues and options.* United Nations Economic Commission for Africa.

English, M. J., Solomon, K. H., & Hoffman, J. G. (2002). A paradigm shift in irrigation management. *Journal of Irrigation and Drainage Engineering*, *128*(5), 267-277.

Duguay,C.R., and Leowe,E.F., (1991) Mapping Surface Albedo in the Eastern Slopes of Colorado Front Range USA with Landsat TM, Artic and alphine Research,volume 23,No.2 May 1991 pp 213-233.

Global Land Cover Facility. (2006). *Earth science data interface*. Retrieved from http://www.glcf.umiacs.umd.edu.8080/esdi/index/jsp

Gowda, P. H., Chavez, J. L., Howell, T. A., Marek, T. H., & New, L. L. (2008). *Surface energy balance based evapotranspiration mapping in the Texas High Plains.* Retrieved from Agricultural Research Service website: http://www.mdpi.org/journal/sensors

Kiama, S. M. (2008). *Exploring application of remote sensing in estimating crop evapotranspiration: Comparison of S-SEBI algorithm and adapted FAO56 model using Landsat TM5 and MODIS* (Master's thesis). ITC Wageningen University, Wageningen, The Netherlands.

Kite, G., & Droogers, P. (2000). Comparing evapotranspiration estimates from satellites, hydrological models and filed data. *Journal of Hydrology*, *229*(1), 1-2. Citied in S. M. Kiama (2008), *Exploring application of remote sensing in estimating crop evapotranspiration: Comparison of S-SEBI algorithm and adapted FAO56 model using Landsat TM5 and MODIS* (Master's thesis). ITC Wageningen University, Wageningen, The Netherlands.

Markham, B. L., & Barker, J. L. (1986). Spectral characterization of the Landsat Thematic Mapper Sensor. *International Journal of Remote Sensing*, *6*(2), 697-716.

Maurer,J.(2006) Retrival of Surface Albedo from Space. Paper written as part of graduate Course in Remote Sensing Field Methods.University of Colorado.

Maxton, A. (2007). *Estimating evapotranspiration using SEBAL.* Retrieved from http://www.gisdevelopment.net/AndrewMaxton/Thesis

Platanov, A., Thenkabul, P. S., Biradar, C. M., Cai, X., Gamma, M., Dheeravath, V., Cohen, Y., Alchanatis, V., Goldshlager, N., Ben-Dor, E., Manthrithilake, H., Kendjabaev, S., & Isaev, S. (2008). *Water Productivity Mapping (WPM) Using Landsat ETM+ data for the irrigated croplands of the Syrdary a river basin in Central Asia*. Retrieved from http://www.mdpi.com/journal/sensors.

Ray, S. S., & Dahwal, V. K. (2001). Estimation of crop evapotranspiration of irrigation command area using remote sensing and GIS. *Agricultural Water Management*, *49*(3), 239-249. Cited in S. M. Kiama (2008), *Exploring application of remote sensing in estimating crop evapotranspiration: Comparison of S-SEBI algorithm and adapted FAO56 model using Landsat TM5 and MODIS* (Master's thesis). ITC Wageningen University, Wageningen, The Netherlands.

Senay, G. B., Budde, M., Verdin, J. P., & Melesse, M. (2007). *A coupled remote sensing and simplified surface energy balance approach to estimate actual evapotranspiration from irrigated fields*. Retrieved from http://www.mdpi.com/journal/sensors

Timmermans,W (1994) "Remote Sensing Evapotranspiration". Delft University of Technology, Faculty of Civil Engineering, Delft.

Tribe, D. (2008). *More crop per drop: Water use efficiency*. Retrieved from http://wwwgmopundit.blogspot.com/2008/06

WaterAid (2007). *Climate change and water resources.* Retrieved from http://www.wateraid.org

Wessling, J. G., & Feddes, R. (2006). Assessing crop water productivity from field to regional scale. *Agricultural Water Management*, *86*(2), 30-39.

ABOUT THE AUTHORS:

Matsa Mark and Muyemeki Luckson are affiliated with the Department of Geography & Environmental Science at Midlands State University in Zimbabwe